Eurasian Journal of Physics and Functional Materials

Volume 9 | Number 2

Article 5

Pages: 104 - 109

6-30-2025

Electrocapacitive properties of cathode materials based on Na3Fe2(PO4)3 polycrystals synthesised by solid-phase and melt-hardening methods

A.A. Nogai
S. Seifullin Kazakh Agrotechnical Research University, Astana, Kazakhstan

E.A. Nogai
S. Seifullin Kazakh Agrotechnical Research University, Astana, Kazakhstan

D.D. Akimbaeva
S. Seifullin Kazakh Agrotechnical Research University, Astana, Kazakhstan

A.S. Nogai
S. Seifullin Kazakh Agrotechnical Research University, Astana, Kazakhstan

A.A. Bush
Russian Technological University MIREA, Moscow, Russia

See next page for additional authors

Recommended Citation

Nogai, A.A.; Nogai, E.A.; Akimbaeva, D.D.; Nogai, A.S.; Bush, A.A.; Tatkeeva, G.G.; and Uskenbaev, D.E. (2025) "Electrocapacitive properties of cathode materials based on Na3Fe2(PO4)3 polycrystals synthesised by solid-phase and melt-hardening methods," *Eurasian Journal of Physics and Functional Materials*: Vol. 9: No. 2, Article 5.
DOI: https://doi.org/10.69912/2616-8537.1246

Electrocapacitive properties of cathode materials based on Na3Fe2(PO4)3 polycrystals synthesised by solid-phase and melt-hardening methods

Authors

A.A. Nogai, E.A. Nogai, D.D. Akimbaeva, A.S. Nogai, A.A. Bush, G.G. Tatkeeva, and D.E. Uskenbaev

ORIGINAL STUDY

Electrocapacitive Properties of Cathode Materials Based on $Na_3Fe_2(PO_4)_3$ Polycrystals Synthesized by Solid-phase and Melt-quenching Methods

Artur A. Nogai [a], Eleonora A. Nogai [a], Dina D. Akimbaeva [a], Adolf S. Nogai [a], Alexandr A. Bush [b], Galia G. Tatkeeva [a], Daniyar E. Uskenbaev [a,*]

[a] S. Seifullin Kazakh Agrotechnical Research University, Astana, Kazakhstan
[b] Russian Technological University MIREA, Moscow, Russia

Abstract

The article provides a comparative assessment of the influence of solid-phase and melt-quenching synthesis methods on the structures and electrochemical properties of $Na_3Fe_2(PO_4)_3$ polycrystals. Solid-phase synthesis of $Na_3Fe_2(PO_4)_3$ polycrystals (1 type of sample) is carried out by a two-stage method according to ceramic technology. In the case of the melt-quenching method of synthesis, firstly, glassy precursors are obtained by melting initial materials under the influence of IR radiation energy and quenching, and after their grinding, pressing, and firing, polycrystals of $Na_3Fe_2(PO_4)_3$ (2nd type of samples) are obtained. In the melt-quenching method, the precursors are obtained under sharp temperature-gradient conditions, and the synthesis of polycrystals occurs rapidly, so the resulting compression strains partially reduce the monoclinic distortions of α-$Na_3Fe_2(PO_4)_3$ structures. Moreover, the degree of crystallinity of type 2 polycrystals is higher than that of type 1 samples. The cathodic electrochemical properties of type 2 samples are found to be significantly higher compared to type 1 samples due to the higher degree of crystallinity and greater symmetry of the α-$Na_3Fe_2(PO_4)_3$ crystal structure.

Keywords: Solid-phase synthesis, Melt-quenching of synthesis, Polycrystals, Structural parameters, Electrical capacitance parameters

1. Introduction

Sodium ion batteries (NIBs) are considered an alternative to in-demand but expensive lithium ion batteries (LIBs), which are used as rechargeable batteries: in electric vehicles, in alternative current sources (as energy storage), etc. However, so far, NIAs are inferior to LIAs in terms of energy capacity and other parameters; therefore, work on increasing their energy parameters is being actively carried out [1—3]. In the future, competitive NIBs can be developed due to the huge availability of sodium and its low cost [2—5]. In recent years, the potential application of ortho and fluoridophosphates in the creation of electrode materials for NIB has already been studied [6,7]. However, the general disadvantage of NIBs is their low energy capacity, which largely depends on the cathode materials. It is necessary to select materials capable of providing high redox potency, good electrochemical capacity, and structural stability during cycling in NIBs [8—10]. Despite the structural stability of cathode materials based on $Na_3Fe_2(PO_4)_3$ during cycling in NIB, the electrochemical capacity in this electrochemical system is not high [8]. The reason for the small electrical capacity of $Na_3Fe_2(PO_4)_3$ based cathodes is its low ionic conductivity in the low-temperature α-phase, due to the monoclinic distortion of the rhombohedral crystal [11]. Therefore, it is necessary to search for new structural materials for NIB cathodes or to develop new technologies and methods to enhance the

Received 5 May 2025; revised 19 May 2025; accepted 22 May 2025.
Available online 30 June 2025

* Corresponding author.
E-mail address: usdan@mail.ru (D.E. Uskenbaev).

https://doi.org/10.69912/2616-8537.1246

conductive and electrochemical properties of existing cathode materials. To increase the ion-conducting properties of $Na_3Fe_2(PO_4)_3$ orthophosphates, melt synthesis methods under the action of concentrated optical and infrared radiation are very effective [12,13]. It was found that the electrochemical properties of cathodes formed based on $Na_3Fe_2(PO_4)_3$ polycrystals obtained by synthesis under the action of concentrated optical radiation have higher electrocapacitive parameters than in the case of samples synthesized by the solid-phase method [14]. However, the electrochemical properties of cathodes formed based on $Na_3Fe_2(PO_4)_3$ polycrystals obtained by the melt-hardening method under the action of infrared radiation have not been tested.

This work aims to investigate the energy parameters of α-$Na_3Fe_2(PO_4)_3$ cathode materials obtained by the synthesis of polycrystals by melt quenching under infrared radiation and to compare these parameters with those of α- $Na_3Fe_2(PO_4)_3$ cathode materials obtained by solid-phase and other methods.

2. Materials and methods of the experiment

2.1. Synthesis of samples

$Na_3Fe_2(PO_4)_3$ polycrystals obtained by two-step solid-phase synthesis are designated type 1 samples. We used the melt-quenching method to obtain $Na_3Fe_2(PO_4)_3$ polycrystals of type 2. For the synthesis of glass-phase $Na_3Fe_2(PO_4)_3$ precursors, a heat-treated mixture of reagents was used, as well as an apparatus consisting of a furnace and a cooling system (refrigerator), which includes a cooled metal housing, rotating blades, and an electric motor. The sample was loaded into the furnace through its side opening, and the melt was drained through the bottom opening of the furnace. The initial sample was suspended in the furnace heated to 950 °C with the help of a platinum grid stand a tungsten holder, and an alundum rod, which was melted within 40–50 s under the action of the energy of the heated furnace and IR radiation from the heating elements. Then the melt was cooled sharply with a cooling device and turned into greyish glassy precursors. Moreover, the density of the glassy precursors exceeded the solid phase precursors. After grinding the glassy precursors, pressing them into tablets, and firing at T = 800 °C for 2 h, polycrystals of $Na_3Fe_2(PO_4)_3$ were obtained. For a comparative analysis of the influence of technological modes of synthesis on the structural and electrochemical properties of $Na_3Fe_2(PO_4)_3$, we will additionally consider the comparison samples synthesized by co-precipitation in Ref. [8].

Technological modes for obtaining polycrystals of $Na_3Fe_2(PO_4)_3$ are given in Table 1.

The data in Table 1 indicate that the synthesis of type 2 samples was accompanied by the highest temperature and sharp temperature gradient effects. Synthesis of type 1 samples was subjected to the longest thermal firings. The comparison samples were subjected to the lowest temperature treatments.

2.2. Polycrystal studies

Structural studies of a polycrystalline sample of $Na_3Fe_2(PO_4)_3$ were carried out using an 8D diffractometer (CuKα radiation) (Bruker). Density studies were carried out using the pycnometric method.

Electrochemical studies of $Na_3Fe_2(PO_4)_3$, type 1 and type 2 polycrystals, were carried out in a three-electrode T-cell. Carbon cloth, chlorosilver electrode, and the investigated materials ($Na_3Fe_2(PO_4)_3$ and others) were used as counter electrode, reference electrode, and working electrode, respectively. Saturated aqueous NaClO4 solution (C ~ 9.2 M) was used as the electrolyte, and a Whatman filter was used as the membrane. The cathode material was prepared by mixing 80 wt. % of the synthesized material, 10 wt. % of Timical C45 carbon as conductive powder, and 10 wt. % solutions of 3 wt. % polyvinylidene fluoride (PVdF) in n-methyl pyrrolidone (NMP) used as binder. Graphite foil (thin graphite foil) was used as a substrate for the cathodes. Cyclic voltammetry (CVA) measurements were performed using a BioLogic CP-300 potentiostat/galvanostat. All measurements were performed relative to a chlorosilver reference electrode.

Table 1. Technological modes for obtaining $Na_3Fe_2(PO_4)_3$ polycrystals by solid-phase and melt-quenching methods.

$Na_3Fe_2(PO_4)_3$ polycrystals		Sample synthesis modes			Ref
Methods of sample synthesis		Firing temperature ^{0} C	Firing time of samples, h	Cooling time, h	
Samples of type 1 were obtained by solid-phase method.	1 firing	600	7	2	
	2 firing	750	7	4	
Samples of type 2 — obtained by melt-quenching method	1 firing	950	0.125	0.82	
	2 firing	750	2	4	
Comparison samples - obtained by co-precipitation method	1 firing	90	2		[8]
	2 firing	600	10	2	

3. Results of the study and their discussion

3.1. Structural data of $Na_3Fe_2(PO_4)_3$ polycrystals

Fig. 1 shows the diffraction patterns of samples of types 1 and 2, which have clear peaks at the corresponding angles.

Note that the peak intensities of $Na_3Fe_2(PO_4)_3$ polycrystal synthesized by the melt-hardening method (type 2 samples) exceed 3 times the corresponding peak intensities of samples obtained by the solid-phase method (type 1 samples). This result may indicate that the degree of crystallinity in type 2 polycrystals is higher than that in type 1 samples, i.e., more crystallites crystallised in type 2 polycrystals than intercrystallite interlayers during synthesis.

Microstructural studies of $Na_3Fe_2(PO_4)_3$ polycrystals of two types, obtained under other technological regimes, can indirectly confirm this assumption [13]. In Ref. [13], it was found that in $Na_3Fe_2(PO_4)_3$ polycrystals synthesized by the melt-hardening method, the density of crystallites significantly exceeded the density of intercrystalline interlayers compared to samples synthesized by the solid-phase method.

Using the Cell Ref program, the diffraction patterns of the samples were indexed and the structural parameters of the unit cell of $Na_3Fe_2(PO_4)_3$ polycrystals were determined, which are presented in Table 2.

The parameters of unit cells of polycrystals of types 1, 2, and samples obtained by the solid-phase method in Ref. [15] presented in Table 2 are close, but there are small differences between them. It should be noted that the unit cell parameters ***a*** of type 2 polycrystals are slightly increased, and the parameters ***b, c,*** and angle ***β*** are slightly decreased compared to the parameters of the type 1 sample. To compare the structural

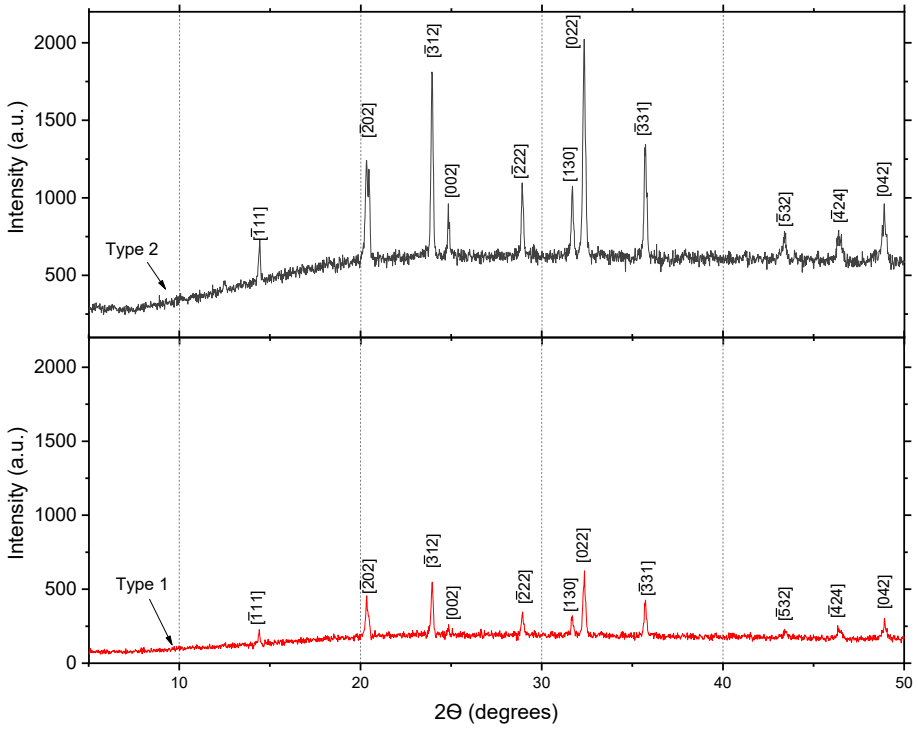

Fig. 1. Diffraction patterns for $Na_3Fe_2(PO_4)_3$ polycrystals obtained by the solid-phase (Type 1) and melt-quenching (Type 2).

Table 2. Unit cell parameters of $Na_3Fe_2(PO_4)_3$ polycrystals.

$Na_3Fe_2(PO_4)_3$ Types of samples	Sp.gr.	Unit cell parameters						Ref
		a, Å	*b*, Å	*c*, Å	α^0	β^0	γ^0	
Type 1st samples	$C2/m$	15.1229	8.7164	21.5962	90.0	90.32	90.0	
Type 2-nd samples	$C2/m$	15.1445	8.6842	21.5766	90.0	90.30	90.0	
Change in structural parameters Δ of type 1 samples relative to type 2		Δ = −0.0216	Δ = 0.0322	Δ = 0.0196	0	Δ = 0.02	0	
Samples obtained by solid-phase method	$C2/m$	15,134	8723	21,571	90.00	90.13	90.0	[15]
Samples obtained by coprecipitation method	$C2/m$	15,346	8744	21,644	90.00	90.03	90.0	[8]

parameters of type 1 and type 2 samples, the parameters of unit cells of $Na_3Fe_2(PO_4)_3$ polycrystals obtained by co-precipitation at lower temperatures (at 600 °C for 10 h) were added to the table since more reactive initial reagents were used as reagents [8]. The table shows that the structure of the samples obtained by co-precipitation has comparable but higher parameters of unit cells ***a, b, c***, and the minimum value of the angle ***β*** in comparison with polycrystals of types 1 and 2. Probably, these features of the structural parameters of the comparison samples are caused by the fact that they were not subjected to high-temperature influences during synthesis.

Thus, comparing the structural parameters of α-$Na_3Fe_2(PO_4)_3$ polycrystals presented in the table, we can conclude that the formation of unit cell parameters of the samples is significantly influenced by the technological modes of their preparation, i.e., the significance of the firing temperature, the duration of heat treatments, the gradients of temperature effects during synthesis.

The changes in the structural parameters of α-$Na_3Fe_2(PO_4)_3$ polycrystals of types 1 and 2, given in Table 2, can be related to additional deformations of unit cells caused by different thermodynamic conditions of synthesis. Probably, insignificant changes in the structural parameters of α-$Na_3Fe_2(PO_4)_3$ type 2 polycrystal obtained by the melt method in comparison with the parameters of the type 1 sample are due to significant uniaxial compression deformation of precursors during their quenching. It is not excluded that the occurrence of mechanical stresses and strains in glassy precursors during sample quenching can be characterized by linear compression (ϵ) according to the law [16]:

$$\varepsilon = \frac{\Delta l}{l} = \alpha \nabla T, \quad (1)$$

where ***α*** is the coefficient of linear compression (or expansion) of the material;

$\varepsilon = \frac{\Delta l}{l}$ - is the relative compression (degree of deformation) of the sample;

$$\nabla T = \frac{dT}{dn} = gradT - \text{temperature gradient},$$

n is the normal direction of the heat flux from the more heated part of the precursor to its cold surface (i.e., to the point of contact between the melt and the quenching device wall).

Although the deformed structures of glassy precursors may be partially reduced during firing, the residual compressive strains (ε) in them may remain significant, since their formation was carried out under conditions of a sharp temperature gradient (between the melt surfaces in contact with the cooling device body and the opposite side). It is possible that the appearance of uniaxial compression strain ε in α-$Na_3Fe_2(PO_4)_3$ type 2 polycrystals contributes to a partial reduction of monoclinic distortions of the crystal structure and a slight increase in the mobility of sodium cations.

3.2. Electrochemical properties of cathodes based on $Na_3Fe_2(PO_4)_3$ polycrystals

All measurements of galvanostatic charge-discharge curves of a $Na_3Fe_2(PO_4)_3$ polycrystal-based cathode with a sodium anode were carried out in a cell with non-aqueous electrolytes and a glove box in an inert atmosphere (Ar) with an oxygen and water content of 0.01 ppm.

Cycling of $Na_3Fe_2(PO_4)_3$ samples in the electrochemical system was carried out at a rate of 0.1C in the voltage range of 1.5–3.5 V. Fig. 3 shows the charge-discharge galvanostatic curves obtained in a cell with sodium anode and cathode based on $Na_3Fe_2(PO_4)_3$ polycrystal.

Fig. 2 shows charge-discharge galvanostatic curves obtained in a cell with a sodium anode and cathode based on polycrystal $Na_3Fe_2(PO_4)_3$. Cycling of $Na_3Fe_2(PO_4)_3$ samples in the electrochemical system was carried out at a rate of 0.1C in the voltage range of 1.5–3.5 V. After long tests, charge-discharge curves were obtained and average charge/discharge capacities were calculated (Table 2). It is known that charge transfer in electrochemical systems is described by the Nernst equation, which relates the potential of the redox process (E) with the standard reduction potential (E_0) and the logarithm of the reaction coefficient, expressed by the activities of the involved particles.

Fig. 3 shows the charge-discharge characteristics of specific capacity (mA g^{-1}) from the number of cycles when tested in the non-aqueous electrolyte of $Na_3Fe_2(PO_4)_3$-based cathode materials.

Fig. 2 shows that the electrocapacitive parameters of cathode materials for type 2 samples are noticeably

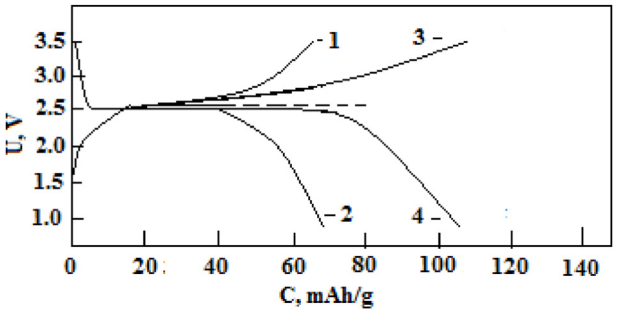

Fig. 2. Charge-discharge galvanostatic curves in non-aqueous electrolyte of $Na_3Fe_2(PO_4)_3$ based cathode materials obtained by solid-phase (curves 1 and 2) and melt-quenching (curves 3, 4) synthesis methods.

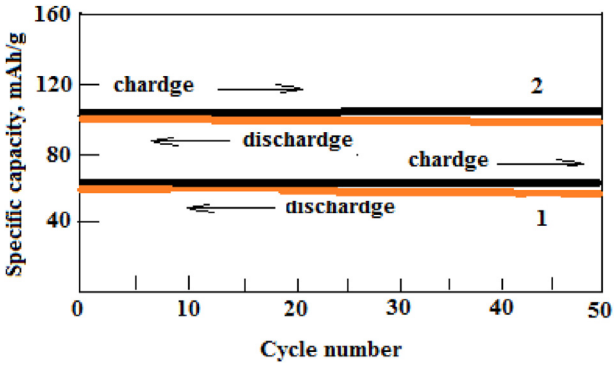

Fig. 3. Dependences of charge/discharge of specific capacity (mA g^{-1}) on the number of cycles when $Na_3Fe_2(PO_4)_3$-based cathode materials are tested in non-aqueous electrolyte: 1 - charge/discharge curves of specific capacitance of cathode materials based on polycrystals of type 1; 2 - charge/discharge curve of specific capacitance of cathode materials based on polycrystals of type 2.

higher than those of type 1 samples. Moreover, according to Fig. 3, both types of samples are characterized by good stability of charge-discharge characteristics at their cyclic operation of 50 times. Reduction of electro-capacitive parameters is not more than 0.9–1 % of the initial value.

Charge transfer in a given electrochemical system can be described by the Nernst equation, which relates the redox potential (E) to the standard reduction potential (E0) and the logarithm of the reaction coefficient expressed by the activities of the involved particles, i.e., iron cations [17].

$$E = E^o + \frac{RT}{F}\ln\frac{a_{Fe^{3+}}}{a_{Fe^{2+}}}, \quad (2)$$

where R is the universal gas constant; T is the absolute temperature; F is the Faraday number; a Fe^{3+} and a Fe^{2+} are the reaction coefficients reflecting the activity of iron cations in the oxidized and reduced processes. Moreover, the standard reducing potential E is determined by the conjugate pair Oh and Red 'oxidant-reductant', i.e., this value is defined as follows:

$$\nu Ox + ne^- \rightarrow \nu' Red, \quad (3)$$

where v, nv'- charges before and after the oxidation-reduction reaction; n - number of electrons. The synthesized samples $Na_3Fe_2(PO_4)_3$ of types 1 and 2 are active for sodium intercalation/deintercalation (presence of reversible Red/Ox peaks), which can proceed by the following reaction:

$$Na_3Fe_2(PO_4)_3 + xNa^+ + xe^- \rightarrow Na_{3+x}Fe^{3+}_{2-x}\,Fe^{2+}_x\,(PO_4)_3 \quad (4)$$

Then the processes of transfer of sodium cations from the cathode to the anode, occurring in the electrocell, can be considered as chemical processes of oxidation at the anode and reduction at the cathode. However, the material is worked through by only 50 % in a non-aqueous medium (from Ste0r = 105 mAh/r), which is a good enough result. In general, the material does not undergo significant degradation when cycling for 50 cycles, in the following it is required to increase the number of cycles to verify the stability of this material. According to the values of specific capacitance of samples of 1 and 2 types, it is possible to calculate the number of charge carriers (n), i.e., the number of sodium ions, participating in electrochemical processes of charge/discharge by the formula [18]:

$$n = \frac{CM}{F}, \quad (5)$$

where C - values of electrochemical cell capacitance; M - molar mass of cathode material; F - Faraday number.

Data on electrochemical tests of $Na_3Fe_2(PO_4)_3$ samples and calculations of para-metre n are given in Table 3. As can be seen from Table 3, cathodes based on samples of type 2 have higher values of electrical capacity (105 mAh/g) than cathodes based on samples of type 1, which indicates the presence of a greater number of sodium cations in the anionic structure of samples of type 2 than samples of type 1 (see the data of Table 3). After long tests, charge-discharge curves were obtained and average charge/discharge capacities were calculated (Table 3).

These data are in agreement with the conclusions of [13] that type 2 polycrystals have higher ionic conductivity than type 1 samples. It should be noted that sodium cations (Na^+) in $Na_3Fe_2(PO_4)_3$ participate more in the reactions of cation intercalation in $Na_3Fe_2(PO_4)_3$in the samples of type 2 than in type 1 (Table 3). Probably, the received data are connected with the fact that the

Table 3. Data on electrochemical tests of $Na_3Fe_2(PO_4)_3$ polycrystals.

Sample types	Method of sample synthesis	Average charge/discharge capacity values mAh/g	Number of charge carriers in charge/discharge processes (n)	Ref
$Na_3Fe_2(PO_4)_3$ Type 1	Solid phase synthesis	64	556	
$Na_3Fe_2(PO_4)_3$ Type 2	Melt- quenching method	105	911	
$Na_3Fe_2(PO_4)_3$	Co-precipitation method	61	530	[8]
$Na_3Fe_2(PO_4)_3$	Sol-gel method	92,5	803	[9]

melt method allows to receive of polycrystals (2 types) of a greater degree of crystallinity than samples of 1 type, which is equivalent to the presence in the specific gravity of cathode material of 2 types of greater concentration of sodium cations. In addition, the electrochemical properties of type 2 samples can be favourably affected by a partial reduction of the monoclinic distortion of the structure of α- α-$Na_3Fe_2(PO_4)_3$ polycrystals, caused by single compression strain, due to sharply gradient-temperature modes of their synthesis.

It should be noted that cathodes based on $Na_3Fe_2(PO_4)_3$ polycrystals synthesized by the sol-gel method demonstrate relatively high specific electrical capacity in NIB [9] due to their high porosity. Despite this, cathodes formed based on $Na_3Fe_2(PO_4)_3$ polycrystals of type 2 can accumulate more specific electrical capacity in NIB, compared to cathodes formed with $Na_3Fe_2(PO_4)_3$ polycrystals obtained by the sol-gel method [9].

Thus, the electrical capacity of $Na_3Fe_2(PO_4)_3$ polycrystals can be significantly increased by using the technology of the melt-quenching method with the use of IR radiation energy.

4. Conclusions

The melt-quenching synthesis method allows to obtaining of polycrystals of α- $Na_3Fe_2(PO_4)_3$ with higher crystallinity and less monoclinic-distorted structures, which have higher electrocapacitive parameters than samples obtained by solid-phase and other synthesis methods. Another advantage of the melt-quenching method of synthesis is a significant reduction of synthesis time compared to the solid-phase method (the time reduction is 5–8 times).

Funding

The work was supported by the Ministry of Science and Higher Education of the Republic of Kazakhstan. Project No. AP 26104305.

Conflict of interest

The authors have no conflict of interests.

References

[1] N. Yabuuchi, K. Kubota, M. Dahbi, S. Komaba, Research development on sodium-ion batteries, Chem. Rev. 114 (2014) 11636–11682, https://doi.org/10.1021/cr500192f.
[2] J.-Y. Hwang, S.-T. Myung, Y.-K. Sun, Chem. Soc. Rev. 46 (2017) 3529–3614, https://doi.org/10.1039/C6S00776G.
[3] T.L. Kulova, A.M. Skundin, Electrochem. Pow. Eng. 16 (3) (2016) 122–150, https://doi.org/10.18500/1608-4039-2016-16-3-122-150.
[4] M.Á. Muñoz-Márquez, D. Saurel, J.L. Gómez-Cámer, et al., Adv. Energy Mater. 7 (2017), 1700463. https://doi.org/10.1002/aenm.201700463.
[5] V. Palomares, P. Serras, I. Villaluenga, et al., Energy Environ. Sci. 5 (2012) 5884–5901, https://doi.org/10.1039/C2EE02781J.
[6] K. Chihara, A. Kitajou, I.D. Gocheva, et al., J. of Power Sources 227 (2013) 80–85, https://doi.org/10.1016/j.jpowsour.2012.10.034.
[7] B. Singh, Z. Wang, S. Park, et al., J. Mater. Chem. A 9 (1) (2021) P. 281–292, https://doi.org/10.1039/d0ta10688.
[8] Y. Liu, Y. Zhou, J. Zhang, et al., ACS Sustain. Chem. Eng. 5 (2017) 1306–1314, https://doi.org/10.1021/acssuschemeng.6b01536.
[9] Y. Cao, Y. Liu, T. Chen, et al., Ionics 25 (3) (2019) 1–8, https://doi.org/10.1007/sll581-018-2804-z.
[10] D. Bin, F. Wang, A.G. Tamirat, et al., Adv. Energy Mater. (31) (2018) 1703008, https://doi.org/10.1002/aenm.201703008.
[11] A.S. Nogai, A.A. Nogai, Stefanovich S. Yu, et al., Phy. Solid State 62 (8) (2020) 1216–1225, https://doi.org/10.1134/S1063783420080259.
[12] A.S. Nogai, A.A. Nogai, D.E. Uskenbaev, et al., Ceramics 6 (4) (2023) 2295–2306, https://doi.org/10.3390/ceramics6040140.
[13] A.S. Nogai, A.A. Nogai, D.E. Uskenbaev, et al., J. Compos. Sci. 8 (14) (2024) 354, https://doi.org/10.3390/jcs8090354.
[14] A.S. Nogai, A.A. Nogai, D.E. Uskenbaev, E.A. Nogai, A.A. Bush, Mat. Sci. Technol. V 2 (2024) 23–29, https://doi.org/10.34920/cce202424 (Chemistry and Chemical Engineering).
[15] V.V. Kravchenko, S.E. Sigaryov, Structural features of the superionic phase transition $Na_3Fe_2(PO_4)_3$, 83, 2, 1992, pp. 149–152, https://doi.org/10.1016/0038-1098(92)90892-D.
[16] I.B. Kopylova, V.V. Neshchimenko, Deformations in Solids. Study Guide, Blagoveshchensk: Amur State University, 2018, p. 15 (in russian).
[17] A.N. Kozitsina, A.V. Ivanova, Yu.A. Glazyrina, et al., Electrochemical Methods of Analysis, Ural Publishing House, Ekaterinburg, 2017, p. 128 (in russian).
[18] V.A. Lipin, A.I. Smirnova, T.A. Sustavova, Physical Chemistry. Electrochemistry: Textbook, St. Petersburg. 2020, p. 94 (in russian).